Electronic Supplementary Information

Nano $AuTiO_{2-x}$ composite with electrochemical characteristics of under-potential deposition of H (H-UPD) as highly efficient electrocatalyst for hydrogen evolution

Zhandong Ren, Lingzhi Jin, Jie Gao, Hanruo Chen, Conghui Zhai, Lingjun Tan, Ning Cong, Hua Fang, Xiaorong Zhou and Yuchan Zhu*

School of Chemical and Environmental Engineering, Wuhan Polytechnic University, Wuhan, 430023, P. R. China.

* Corresponding author:

Yuchan Zhu, Professor, School of Chemical and Environmental Engineering, Wuhan Polytechnic University, Wuhan, 430023, P. R. China.

E-mail: zhuyuchan@163.com. Tel.: 86-27-83943956.

Experimental methods

Nano $AuTiO_{2-x}$ electrode was prepared by simple thermal decomposition method in Scheme S1. In a typical synthesis process, 0.4 mmol tetrabutyl titanate ($Ti(OC_4H_9)_4$) was added to 3.0 mL alcohol (C_2H_5OH) under vigorous stirring using a magnetic stirrer. Then, the pH value of solution was adjusted to 8, and the solution was slowly stirred for 2 h and aged for 24h to form solution A (TiO_2 sol). Subsequently, 0.8 mmol chloroauric acid ($HAuCl_4 \cdot 4H_2O$) was added to 3.0 mL alcohol (C_2H_5OH) to form solution B. Solution A and B were mixed according to the volume ratio of 1:1 and stirred at room temperature for 1 h to obtain a clear and transparent orange Au-TiO_2 composite precursor sol. Next, 50 μL of the mixed solution was uniformly dropped on the surface of carbon paper (CP) (pretreated in HNO_3 for 12 h) and dried naturally. The above coating process was repeated 6 times until the loading of Au on CP was about 15 mg cm^{-2}. Finally, the sample was annealed at 500 ℃ for 2h at a heating rate of 5 ℃ min^{-1} in Ar atmosphere. Au electrode were prepared by the same thermal decomposition method described above except that solution A was not added. Pt electrode were prepared by the same thermal decomposition method described above with H_2PtCl_6 solution.

X-ray diffraction (XRD) patterns were acquired on an XRD-7000 X-ray diffractometer. Transmission Electron Microscopy (TEM) were conducted on an JEOL-2100F. Scanning Electron Microscope (SEM) images were taken with a Zeiss ΣIGMA field-emission SEM. X-ray photoelectron spectrometry (XPS: ESCLAB 250Xi, Thermo Scientific) with monochromatized Al Ka radiation was used to analyze the electronic properties. Analysis of the composition of the electrode was carried out by X-ray fluorescence (XRF: EDX-7000, Shimadzu, Japan).

The electrochemical experiments were carried out in a typical three-electrode electrochemical glass cell with a carbon paper as a counter electrode and $Hg/Hg_2SO_4/K_2SO_4$(0.1 M) as the reference electrode. Cyclic voltammetry (CV) measurements were performed in Ar-saturated 0.5 M H_2SO_4 solution at the scan rate of 100 mV s^{-1}. The HER polarization curves were obtained by sweeping at a scan rate of 5 mV s^{-1}. Electrochemical impedance spectra (EIS) were recorded at overpotentials of 80 mV with the frequency ranging from 100 mHz to 100 kHz with a constant ac voltage amplitude of 10 mV.

First-principles calculations were performed using the Vienna Ab Initio Simulation Package (VASP, version 5.3) within a RPBE (Revised Perdew Burke Ernzerhof) generalized gradient approximation (GGA) to the exchange and correlation functional. A projector augmented wave (PAW) basis along with a plane-wave kinetic energy cutoff of 408 eV was employed for all computations. During the geometry optimization, the adsorbate layer and the top three layers of the slab were allowed to relax. The energies were converged to 1×10^{-3}eV per atom and ionic relaxations were allowed until the absolute value of force on each atom was below 0.02 eV/A. $AE_H = E(H/M) - E(M) - 1/2E(H_2)$, such that the negative value indicates the dissociation of H_2 on the studied surface being thermodynamically spontaneous, whereas the positive means the opposite.

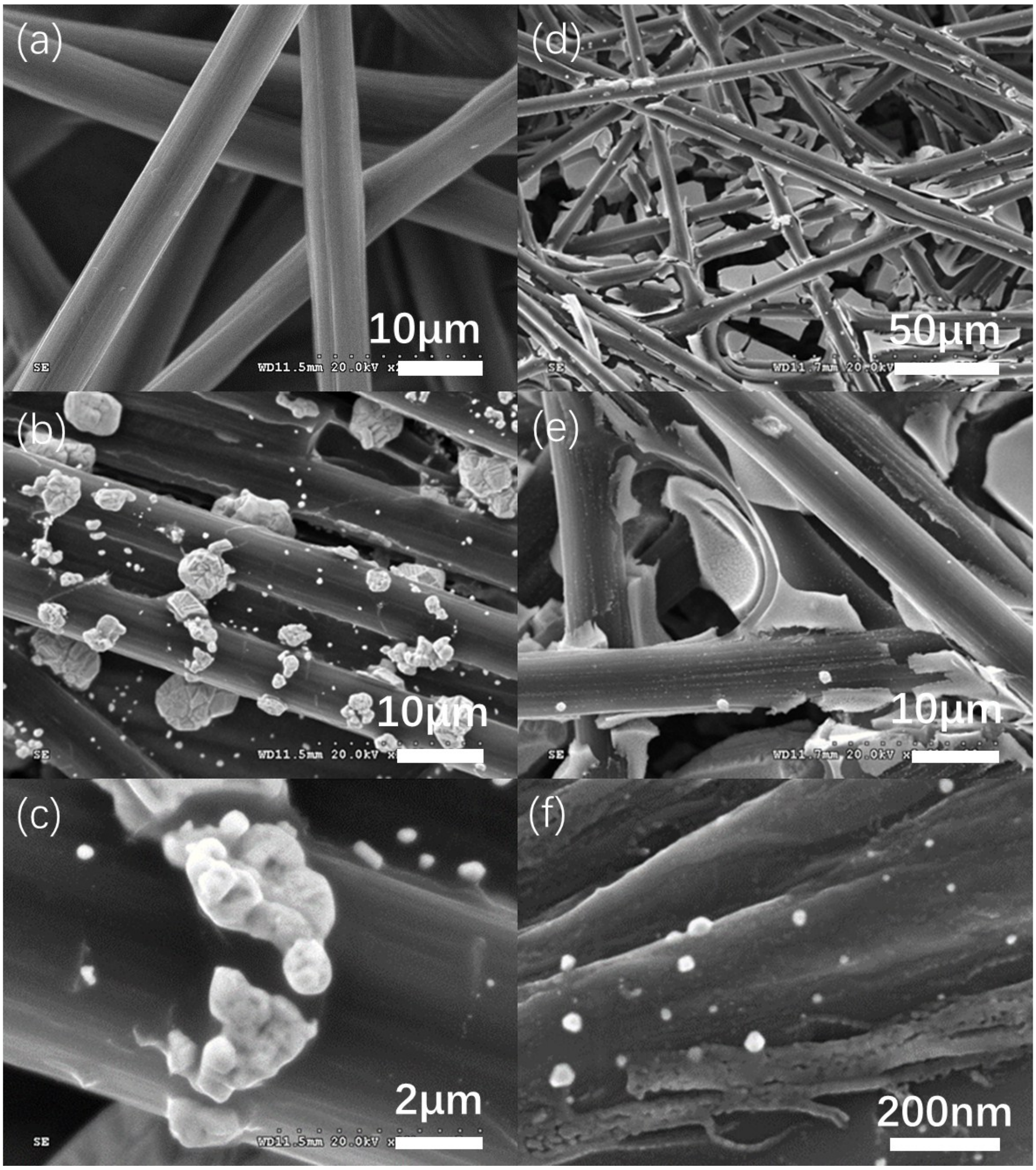

Figure S1 SEM images of CP (a), Au/CP (b, c) and AuTiO_{2-x}/CP (d-f).

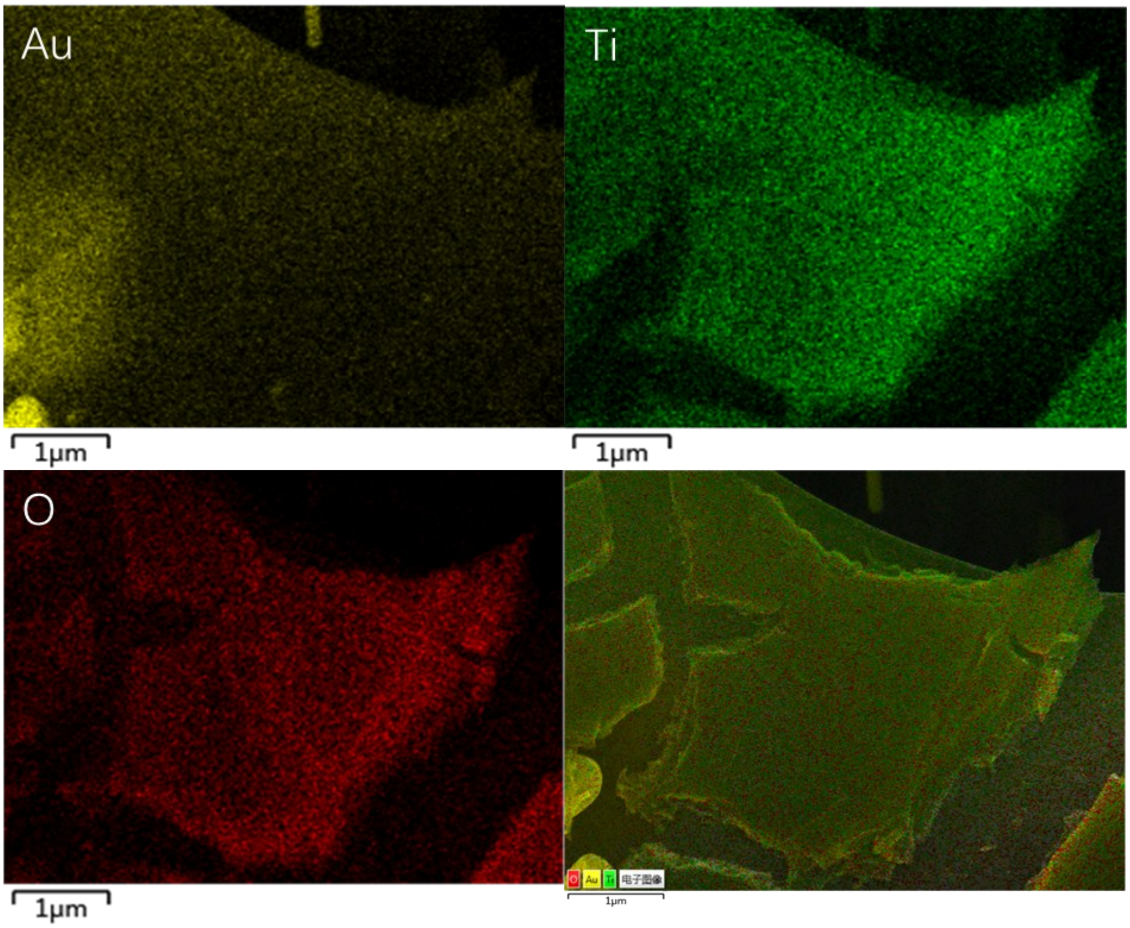

Figure S2 SEM-EDS elemental maps (Au, Ti and O) of AuTiO$_{2-x}$ nanoparticles.

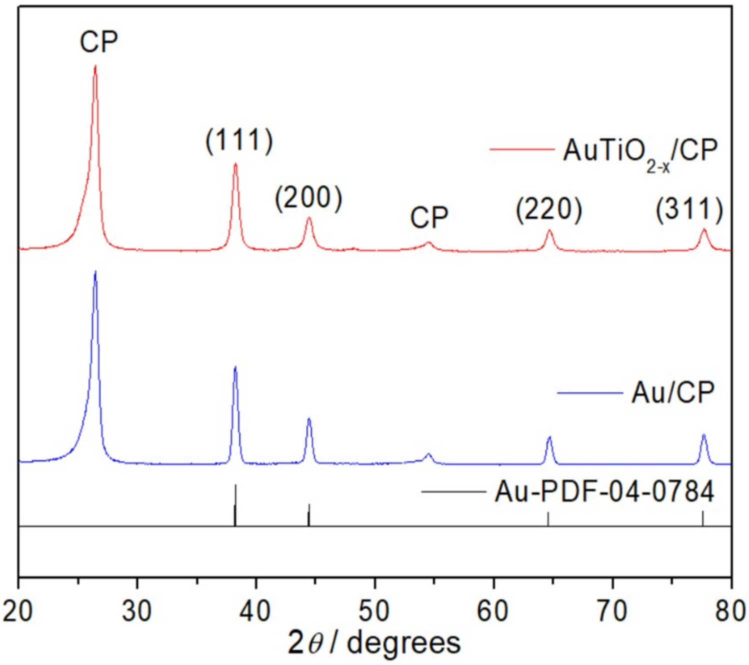

Figure S3 XRD images of Au and AuTiO_{2-x} nanoparticles.

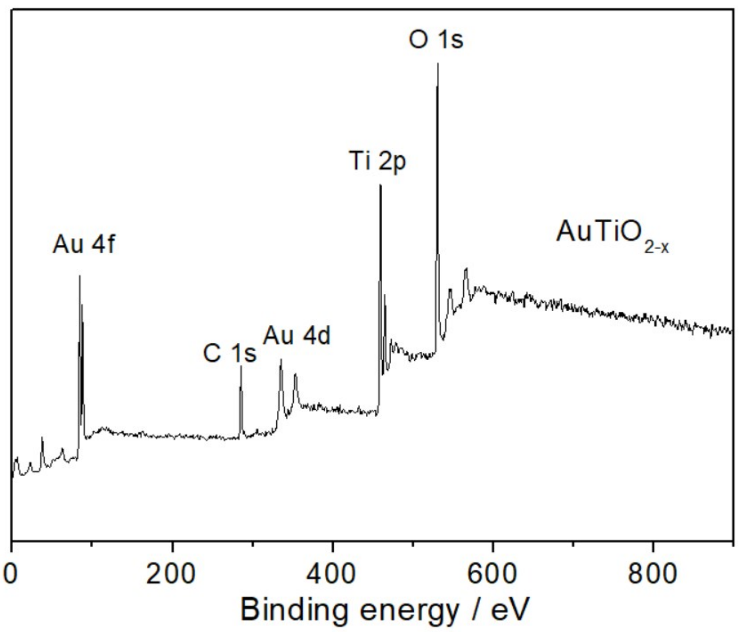

Figure S4 The XPS survey spectrum of AuTiO$_{2-x}$ electrodes.

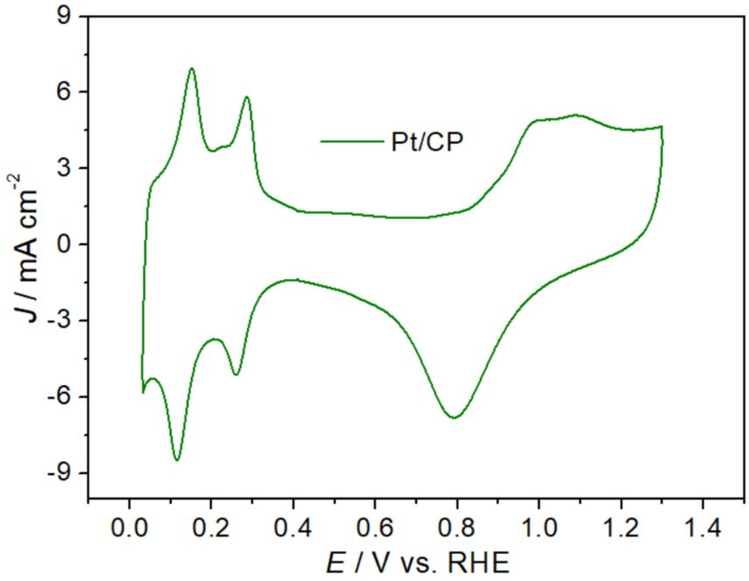

Figure S5 The cyclic voltammogram (CV) of the Pt electrode.

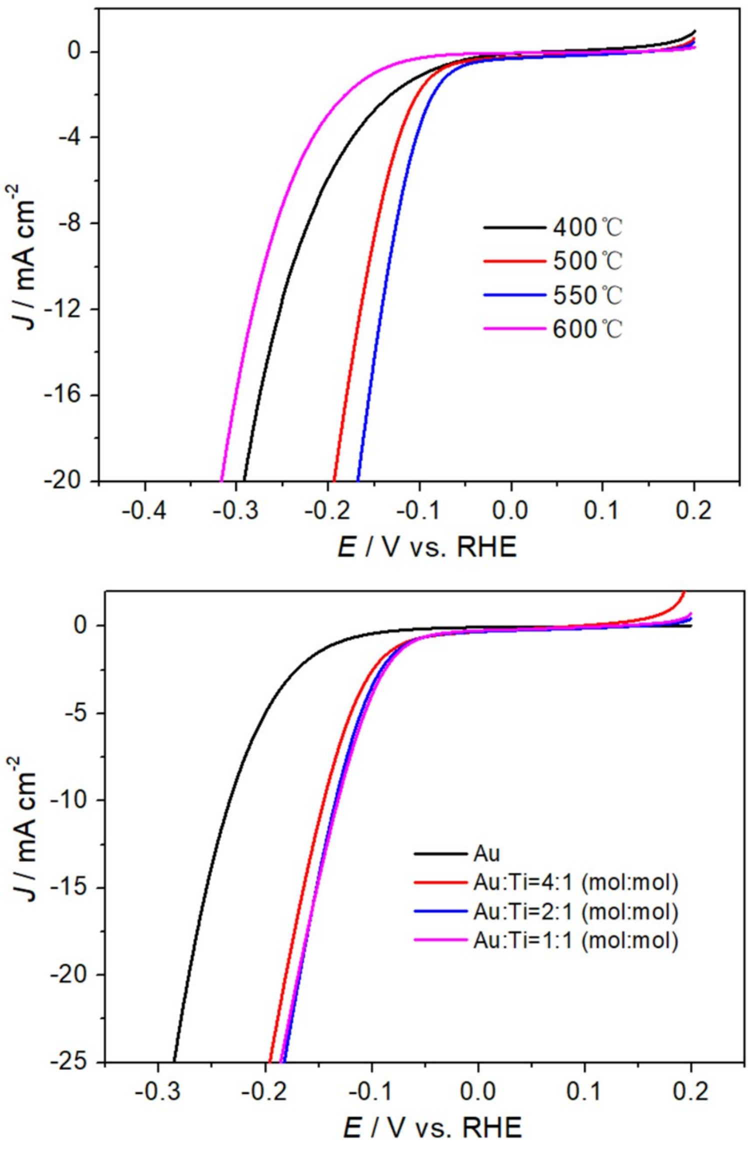

Figure S6 The HER activities of $AuTiO_{2-x}$ electrodes with different calcination temperatures and Au-Ti mole ratios.

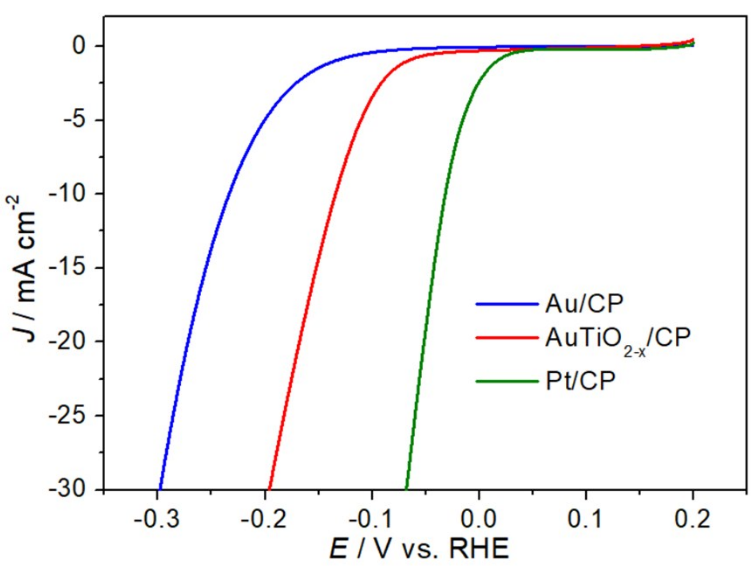

Figure S7 The HER activities of $AuTiO_{2-x}$, Au and Pt electrodes.

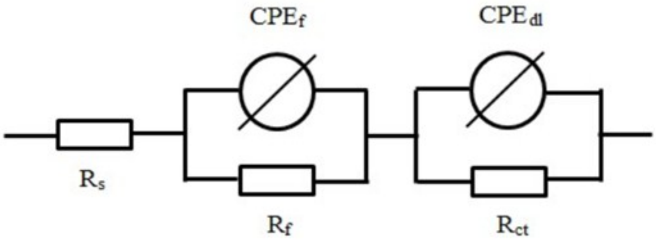

Figure S8 The equivalent circuit of the impedance of AuTiO$_{2-x}$ and Au electrodes

Table S1 ED-XRF analysis of $AuTiO_{2-x}$ electrode before and after stability tests

Electrode	Au / mol%	Ti / mol%
$AuTiO_{2-x}$	47.69	52.31
$AuTiO_{2-x}$ after 1000 segments CV	45.48	54.52
$AuTiO_{2-x}$ after10000s @-0.15V	48.30	51.70

Table S2 The activity and stability of Au nanohybrids catalysts for HER in acid medium

Catalyst	Active center	j (mA cm^{-2}) @ potential (mV)	η (mV) @ current density (mA cm^{-2})	Tafel slope (mV dec^{-1})	Stability	Ref.
Au-Mo_2N particles①	Au and Mo_2N	---	200@ 10	67	---	1
Au-MoS_2 nanosheet②	---	---	289 @ 10	68	---	2
Au-Mo_2N②	Au and Mo	0.29 @ 250	---	106 ± 4	---	3
Au-Mo_2N-BP②	Au and Mo	2.43 @ 250	---	63 ± 3	---	
Au-aerogel-CN_x composites②	Au and CN_x	---	185 @ 10	53	The J reduced by 30% at η = 150 mV after 10h	4
MoS_2–Au nanohybrids②	MoS_2 (Au: conductivity)	---	66 @ 10	40	The J reduced by 11% decrease at η = 70 mV after 12h	5
WS_2/Au hybrids ②	WS_2 (Au: conductivity)	14.5 @ 400	---	57.49	---	6
MoS_2/Au hybrids②	MoS_2 (Au: conductivity)	22.6 @ 400	---	56.97	---	
Core/Shell NiAu/Au②	NiAu/Au	---	---	36	---	7
Au@Zn-MOF③	Au@Zn-MOF	1.5 @ 100	---	86.5	---	8
Au-Ag icosahedra	Au-Ag	---	---	39	---	9
AuTiO_{2-x}②	Au	3.5 @ 100 32 @ 200	134 @ 10	60.34	No change after 10000s @150 mV.	This work

Electrolyte Solution: ①0.1 M H_2SO_4, ②0.5 M H_2SO_4, ③0.1 M $HClO_4$.

1 A. Morozan, V. Goellner, A. Zitolo, E. Fonda, B. Donnadieu, D. Jonesa, F. Jaouen, *Phys. Chem. Chem. Phys.*, 2015, **17**, 4047-4053.
2 D. Hu, Y. Shi, Y. Du, W. Yu, J. Huang, H. Gao, M. Zhu, *Polymer*, 2018, **153**, 331-337.
3 U. Joshi, J. Lee, C. Giordano, S. Malkhandi, B.S. Yeo, *Phys. Chem. Chem. Phys.*, 2016, **18**, 21548-21553.
4 M.K. Kundu, T. Bhowmik, S. Barman, *J. Mater. Chem. A*, 2015, **3**, 23120-23135.
5 J. Zhang, T. Wang, L. Liu, K. Du, W. Liu, Z. Zhu, M. Li, *J. Mater. Chem. A*, 2017, **5**, 4122-4128.
6 J. Kim, S. Byun, A. J. Smith, J. Yu, J. Huang, *J. Phys. Chem. Lett.*, 2013, **4**, 1227-1232.
7 H. Lv, Z. Xi, Z. Chen, S. Guo, Y. Yu, W. Zhu, Q. Li, X. Zhang, M. Pan, G. Lu, S. Mu, S. Sun, *J. Am. Chem. Soc.*, 2015, **137**, 5859-5862.
8 D.K. Yadav, R. Gupta, V. Ganesan, P.K. Sonkar, M. Yadav, *ChemElectroChem*, 2018, **5**, 2612-2619.

9 Y. Qin, X. Dai, X. Zhang, X. Huang, H. Sun, D. Gao, Y. Yu, P. Zhang, Y. Jiang, H. Zhuo, A. Jin, H. Wang, *J. Mater. Chem. A*, 2016, **4**, 3865-3871.

Table S3 Impedance parameters of $AuTiO_{2-x}$ and Au electrodes obtained by fitting the experimental data to $R_s(R_fC_f)(R_{ct}C_{dl})$ equivalent circuit

Electrocatalyst	R_s /Ω cm^2	R_f /Ω cm^2	C_f /μF cm^{-2}	R_{ct} /Ω cm^2	C_{dl} /mF cm^{-2}
$AuTiO_{2-x}$	0.78	0.78	2.69	51.21	9.56
Au	0.38	1.32	0.97	210.6	0.0246